A GRS METHOD FOR PARETO-OPTIMAL FRONT IDENTIFICATION IN ELECTROMAGNETIC SYNTHESIS

♯ Marco Farina, ♭ Alessandro Bramanti, ♭ Paolo Di Barba

♯ STMicroelectronics
Via C. Olivetti 2, 20041 Agrate Brianza (MI), IT.
marco.farina@st.com

♭ University of Pavia, Department of Electrical Engineering
Via Ferrata 1, 27100 Pavia, IT
di_barba@unipv.it, bramanti@etabeta.unipv.it

June 10, 2002

Abstract

Though optimization problems in industrial electromagnetic design are often truly multiobjective, solving them by evolutionary Pareto Optimal Front approximation is often unpractical, due to the high computational cost of objective evaluations. In order to overcome this drawback, an extension of classical single-objective Generalized Response Surface (GRS) methods to Pareto-optimal front approximation is proposed. Such an extension implies essential modifications, due to the increased complexity of multiobjective optimization problems.

Neural network (NN) interpolation, Pareto evolutionary search and special zooming strategies are combined in an iterative procedure, that leads to a strong reduction in true objective function calls.

After a brief formal presentation of multiobjective optimization problems, and an overview of the utility of such an approach in electromagnetic design, a description of the proposed methodology is given and an electromagnetic test case is presented and solved, in order to show the validity of the strategy.

1 Introduction

GRS methods are a well established technique for single-objective optimization, in case of time consuming objective function evaluation. The essential idea is to consider two different objective functions, i.e. the true function is computed, to provide values for a subsequent interpolation (interpolated objective function). Since computation is costly for the true function, and virtually inexpensive for the interpolated, calls to the former should be kept as few as possible. Yet, as also precision is required in retrieving the solution, iterative enhancement

of the interpolation is often included, which adds points in the most likely interesting or worst defined zones of the surface. Polynomials, multiquadrics and neural networks are some examples of the interpolating techniques used, and the 'virtual' objective function they provide, can be called by the optimization algorithm.

In fact, in the literature, many Response Surface Methods are documented [1, 2, 3, 4], coupling especially the aforementioned approximation techniques with stochastic algorithms, such as genetic or evolutionary. Evolutionary Multi-objective Optimization (EMO), on the other hand, is a well established computational research area, whereby several powerful methods are available for POF approximation ([5],[6]). The relevance of the possible link between EMO methods and GRS strategies is evident, thinking of the high computational costs of Multi-objective Evolutionary Algorithms (MOEAs), which may become impractical when industrial design is concerned [7].

2 Pareto Multi-objective Optimization Problems: Mathematical Aspects

The following nonlinear constrained multi-objective optimization problem (MOP) will be considered throughout the paper assuming, without loss of generality, that all objectives are to be minimized; for a detailed and rigorous mathematical theory of MOPs see [8]:

$$\begin{cases} \min\limits_{\mathbf{x}\in\mathbb{R}^N} & \mathbf{f} = \{f_1(\mathbf{x}), ..., f_M(\mathbf{x})\} \\ subject\ to & \mathbf{g}(\mathbf{x}) \leq 0 \\ & \mathbf{h}(\mathbf{x}) = 0 \end{cases} \tag{1}$$

Problem 1 gives rise to the following subspaces, known as design domain and objective domain search spaces, respectively:

$$\begin{array}{c} \Omega \ : \ \{\mathbf{x} \in \mathbb{R}^N \ s.t. \ \mathbf{g}(\mathbf{x}) \leq 0 \ and \ \mathbf{h}(\mathbf{x}) = 0\} \\ \Omega_O \ : \ \{\mathbf{f}(\mathbf{x}) \in \mathbb{R}^M \ s.t. \ \mathbf{x} \in \Omega\} \end{array} \tag{2}$$

Ω_o being the image of Ω through function $\mathbf{f}$. In order for problem 1 to be non-trivial, the following condition is to be imposed:

$$\nexists \, \mathbf{x}_U \in \Omega \ s.t. \ f_i(\mathbf{x}_U) = \min_{\mathbf{x}\in\Omega} f_i(\mathbf{x}) \quad \forall i = 1 : M \tag{3}$$

that is, no points in Ω minimize all objectives at the same time (no cooperative objectives). When such a problem is tackled, a proper definition of optimality is to be considered. It is common in engineering problems to use Pareto optimality and we will do it as well, but other possible definitions may be considered (see for example Nash optimum definition and its applications in [9]). The following two definitions give the concept of Pareto-better (Pareto-dominating) solution and Pareto-optimal solution:

Def 2.1 *For any two points (candidate solutions)* $\mathbf{x}_1, \mathbf{x}_2 \in \Omega$, $\mathbf{x}_1$ *is said to* dominate $\mathbf{x}_2$ *in the Pareto sense if and only if the following conditions hold:*

$$\begin{cases} f_i(\mathbf{x}_1) \leq f_i(\mathbf{x}_2) & \text{for all } i \in \{1, 2, ..., M\} \\ f_j(\mathbf{x}_1) < f_j(\mathbf{x}_2) & \text{for at least one } j \in \{1, 2, ..., M\} \end{cases}$$

Def 2.2 $\boldsymbol{x}^* \in \Omega \, is \, Pareto-optimal \, (PO) \, if \ \nexists \, \boldsymbol{x} \in \Omega \, s.t. \, f_i(\boldsymbol{x}) \leq f_i(\boldsymbol{x}^*) \, \forall i = 1 : M \, and \, f_j(\boldsymbol{x}) < f_j(\boldsymbol{x}^*) \, for \, at \, least \, one \, j \in [1 : M]$

As a consequence of definition 2.2 the number of solutions of problem 1 is infinite, and we call Pareto-optimal set (POS) and Pareto-optimal front (POF) the following two subspaces respectively:

$$\begin{array}{c} POS = \{\mathbf{x}^* \in \Omega \; s.t. \; \mathbf{x}^* \; is \; PO\} \\ POF = \{\mathbf{f}(\mathbf{x}^*) \in \Omega_O \; s.t. \; \mathbf{x}^* \in POS\} \end{array} \tag{4}$$

The following two points in the objective space domain Ω_O

$$\mathbf{U} = \left[\min_{\mathbf{x}\in\Omega} f_i\right] \quad i = 1 : M \tag{5}$$

$$\mathbf{D} = \left[\max_{\mathbf{x}\in\Omega} f_i\right] \quad i = 1 : M \tag{6}$$

are known as Utopia and Distopia point respectively; they give some very preliminary information about Ω_O itself.

As a consequence of statement 3, the inverse image of $\mathbf{U}$ does not belong to Ω and $\mathbf{U}$ does not belong to Ω_O.

From the point of view of application in electrical engineering shape design, we consider the following classification of problems:

- A single Pareto-optimal solution is required without any preference on objectives,
- A single Pareto-optimal solution is required with some preference on objectives,
- n Pareto-optimal solutions are required (a sampling of the POF).

The method we consider in this paper is devoted to the solution of problems belonging to the third class, and presenting time consuming evaluation of one or more objectives.

3 Pareto Multi-objective Optimization problems in electromagnetic design

The degree of complexity of design problems in electrical engineering asks for sophisticated models and robust algorithms to solve both direct and inverse problems. In particular, the latter naturally are multiobjective problems and imply the simultaneous minimization of conflicting objectives subject to suitable constraints. A typical case is to minimize weight and materials cost or to maximize some output of the device, taking into account physical constraints and geometrical bounds. It should be recognized that the presence of a single objective is somewhat an exception or a simplification. Often, constraints are nothing but hidden objectives; always, the fabrication tolerance of a device represents an objective being in conflict with the device performance. From the designer viewpoint, there are numerous benefits coming from the approach to the design in terms of multiobjective optimisation. First, a wide choice among best compromises implies a better compatibility of the design with industrial normalization and technological constraints; the latter, in fact, are difficult to be prescribed *a priori* in an exhaustive way. Moreover, having a set of optimal solutions makes it easy to fulfil *a posteriori* time-varying constraints that are typical of real-life engineering; an example could be the actual availability of materials, depending in turn on the flow imposed by suppliers. On the other hand, in scalar optimization all constraints have to be carefully prescribed in order for the only solution to be feasible. Finally, multi-objective optimization enhances the diversity of performances among best compromises and, therefore, could highlight non-trivial designs that are *a priori* unpredictable even by an experienced designer.

4 Extending GRS methods to Pareto-optimal front identification

Generalized Response Surfaces (GRS) methods are a well established technique for single-objective optimization [10, 11] in case of time consuming objective function evaluation. The essential idea of such methodologies is to handle any of the objective functions in two different fashions. The first one is the true function which is to be evaluated as few times as possible, due to its computational cost. The second one is the interpolation of the true objective function via a suitable technique (polynomials, multi-quadrics [10, 11], neural networks [12]) and its evaluation can be considered inexpensive. A global search algorithm (GA, ES, SA, DE) can be run on the interpolated function up to full convergence. Moreover an iterative strategy, alternating search of a new optimum and enhancement of the interpolation in the current optimum region, is performed. The aim of single-objective GRS methods is to increase convergence speed on one hand, and to improve interpolation in the area of current optimum only, with a dramatic reduction in the number of experiments, on the other hand. The extension of such a strategy to POF approximation is considered in the following. The general structure of a GRS method for multiobjective optimization is essentially similar to the single-objective counterpart. The location of new points in the design domain, is chosen by means of an auxiliary function.

The proposed GRS-MOEA is based on NN-interpolation; its main steps are here summarized [13]:

Step 1
- If the design domain is an n-dimensional box, build an initial training set $[X]$ as an n-dimensional regular p^n points grid, where p is the number of points in each edge of the n-dimensional search space. On the other hand, if the search space is bounded by nonlinear constraints, a design of experiments strategy for the choice of $[X]$ is to be used; the cost of this step is N_I .
- Evaluate the true objective functions for all points on the set in order to build the first training values array $[F]$.

Step 2 Build the first NN interpolation $F_{NN}(0)$ using all training nodes and values of step 1.

Step 3
- Start an iterative procedure, t being the iteration counter. If $\langle t, k_a \rangle$=0 (k_a being a parameter to be defined $\approx$ 2-10) add a node $\mathbf{x}^*$ (information point) in the interpolation nodes set $[X]$ in the most unexplored area of the whole search space, and compute the true objectives values $F(\mathbf{x}^*)$ for that point. The contribution of this block to the cost is 1. The addition of information points increases the probability of jumping out of possible local fronts and requires an optimization in itself.
- On the other hand, if $\langle t, k_a \rangle \neq$0 run a MOEA on the current NN-interpolated functions $F_{NN}(t)$ and obtain a current solution set $[X_P]$ for the interpolated functions;
- extract non-dominated solutions (see section 2 for the definition) and obtain the set $[X_P^d]$,
- select some solutions discarding those that are too close in design space and obtain $[X_P^{dc}]$;
- compute true objective functions $F([X_P^{dc}])$; this block costs $N_P^{DC}(t)$.
- update the search space in the design domain (see below for details).

Step 4 If the termination criterion is satisfied stop the search, otherwise add $[X_P^{dc}]$ and $F([X_P^{dc}])$ to the training set and values and build an updated NN-interpolated functions $F_{NN}(t+1)$; after that go to the next iteration .

The flowchart of the described methodology is shown in figure 1. The true objective function

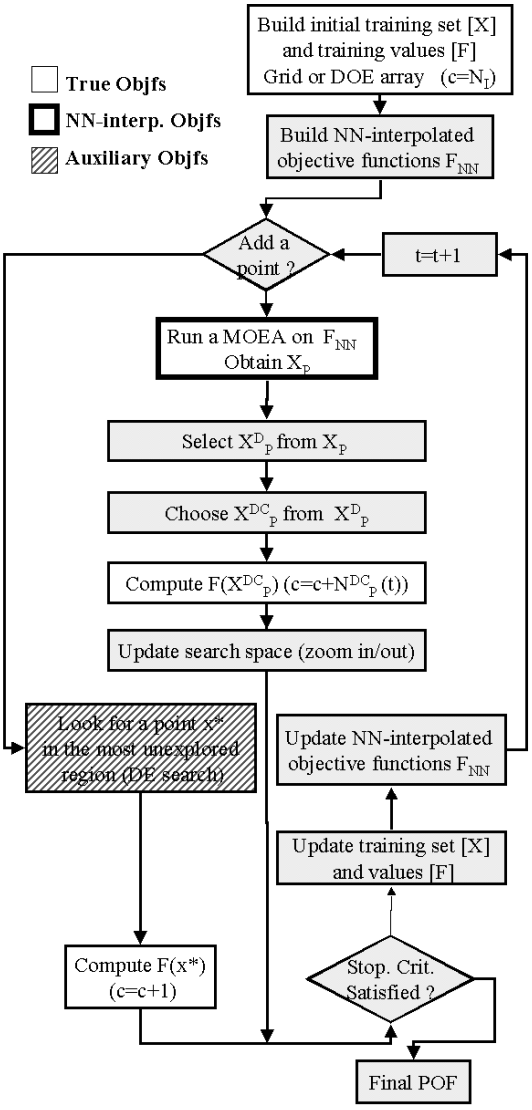

Figure 1: Principle flowchart of the proposed NN-based GRS-MOEA; the use of three different objective function for each criterion is outlined together with the contribution of each block to the cost c.

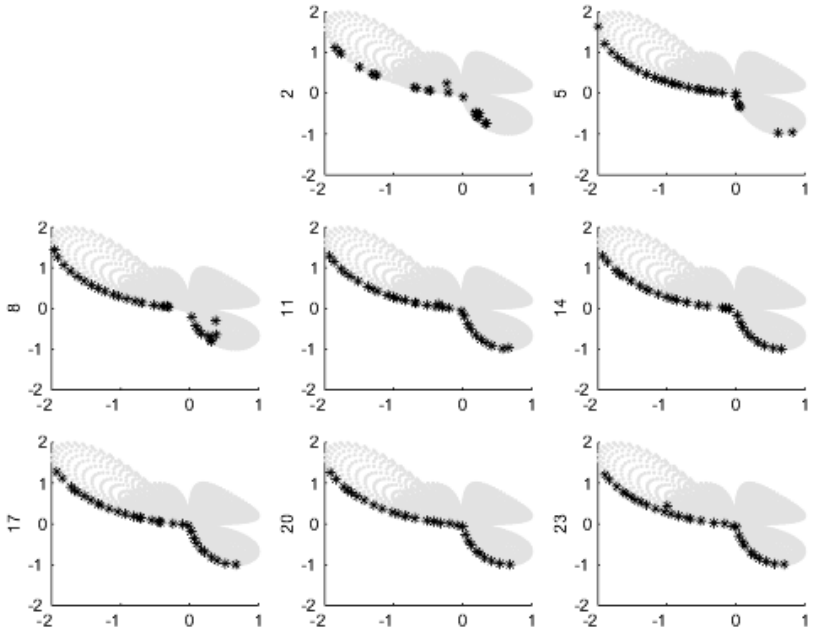

Figure 2: Behavior of the proposed GRS-MOEA strategy on a test problem (see [13] for equations) in the objective domain (two objectives); black $*$: current POF, gray dot: search space sampling (the overall iteration number is marked on the left) .

evaluation number (cost of the algorithm) up to iteration $\widetilde{t}$ can be evaluated as follows:

$$c(\widetilde{t}) = N_I + \sum_{\substack{t=1 \\ \langle t, k_a \rangle \neq 0}}^{\widetilde{t}-1} [size(X_p^{dc}(t))] + \frac{\widetilde{t}-1}{k_a} \tag{7}$$

where the third term gives the cost of the information point addition and the $\langle \cdot, \cdot \rangle$ is intended as the modulus function.

The task of updating the current search space when the overall iterative process goes on is much more complex for a multiobjective problem than for the single-objective counterpart. In the latter case the current optimum region can be easily defined as an n-dimensional cube or sphere centered in the current optimum point; it is therefore easy to perform a zooming procedure in such a situation. When a multiobjective problem is concerned the current set of non-dominated solutions is a general (sometimes disconnected) n-dimensional set in the design domain and a proper zooming strategy is to be carefully considered (see [13] for details).

When the term "cost" is used, the number of true objective function evaluation is intended; moreover we point out that, in order to save computational efforts, all points where the true objective functions are computed, are added to the NN training set; $c(t)$ for $0 < t < \widetilde{t}$ is thus the NN training cost at iteration t. At each iteration a new NN interpolation is built on the current training set. On the other hand, as can be seen easily from the flowchart, the pseudo-cost (number of NN-interpolated function evaluations) is extremely high, but its time requirement is supposed to be negligible with respect to the cost (the case of very time consuming true objective function evaluation is always considered).

Moreover, the cost does not depend on the number of desired solutions on the POF and on the population size of the MOEA in step 3.

The updating of the search space in design domain is non-trivial with respect to the single-objective counterpart. The POS region may be connected or disconnected.

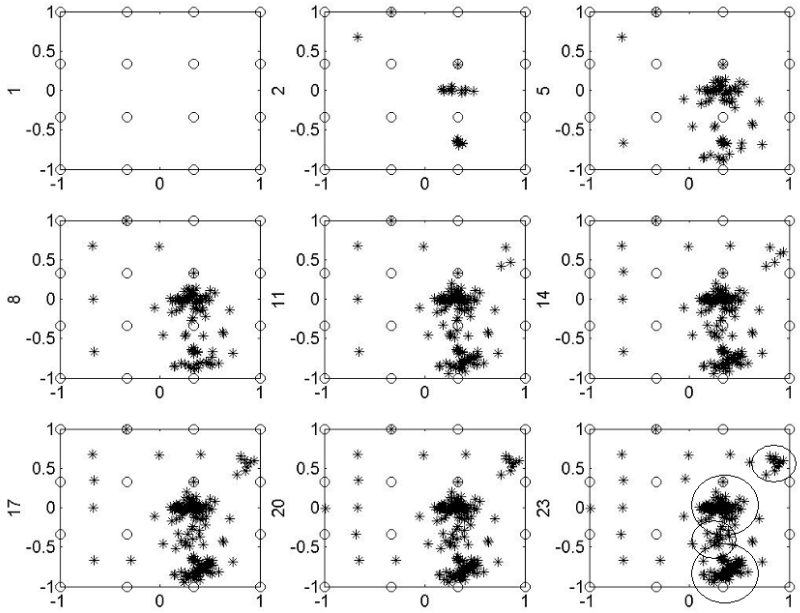

Figure 3: Behavior of the proposed GRS-MOEA strategy on a test problem (see [13] for equations) in the design domain (two design variables); $\circ$: initial NN-training grid, $*$: current solution (the overall iteration number is marked on the left).

In the first case an n-dimensional box, centered on the center of weights of the current POS, can be considered. In the second case the sum of different boxes centered on centers of weight of all parts of the POS is to be used. As an example, a test problem where this second strategy is to be used, is shown in figure 3 (design domain) and 2 (objective domain). The POS is a set of disconnected regions while the POF is non-convex but connected. As can be seen the both the POS and POF are properly sampled with a satisfactory number of solutions;

The choice of a point in the most unexplored area of the search space, to be added to interpolation set, can be performed via an auxiliary optimization procedure (see details in [11], but could also be substituted by a suitable DOE strategy for the evaluation of the most unexplored area in the search space. Moreover the choice of NN as interpolation technique is of course arbitrary and other techniques could also be done, such as multiquadrics or polynomial functions. The power and flexibility of NN with respect to other techniques was outlined in previous studies on GRS methods for single-objective problems [10, 11]. From this point of view the proposed method behaves in a similar way to single-objective GRS methods. On the other hand, when the proposed method is considered the quality of approximation is to be evaluated on the resulting POF and not on the single interpolated objective functions.

5 Electromagnetic test-case

An electromagnet composed of an excitation winding included in a fixed magnetic core and a plunger, representing the movable core, is considered. The cross section of the device, exhibiting a translational symmetry, is shown in Figure 4a. The electromagnetic force acting on the plunger appears when the winding is supplied a rectangular pulse of magneto-motive force, corresponding to a current density of $J = 2 \cdot 10^5$ $[A/m^2]$ for a duration of 80 [ms]. The current-carrying conductor has a diameter small with respect to penetration depth, and is wound up to form a stranded winding; moreover, a rough calculation shows that the power loss due to eddy currents in the plunger is much smaller than the Joule power loss in the winding. Therefore

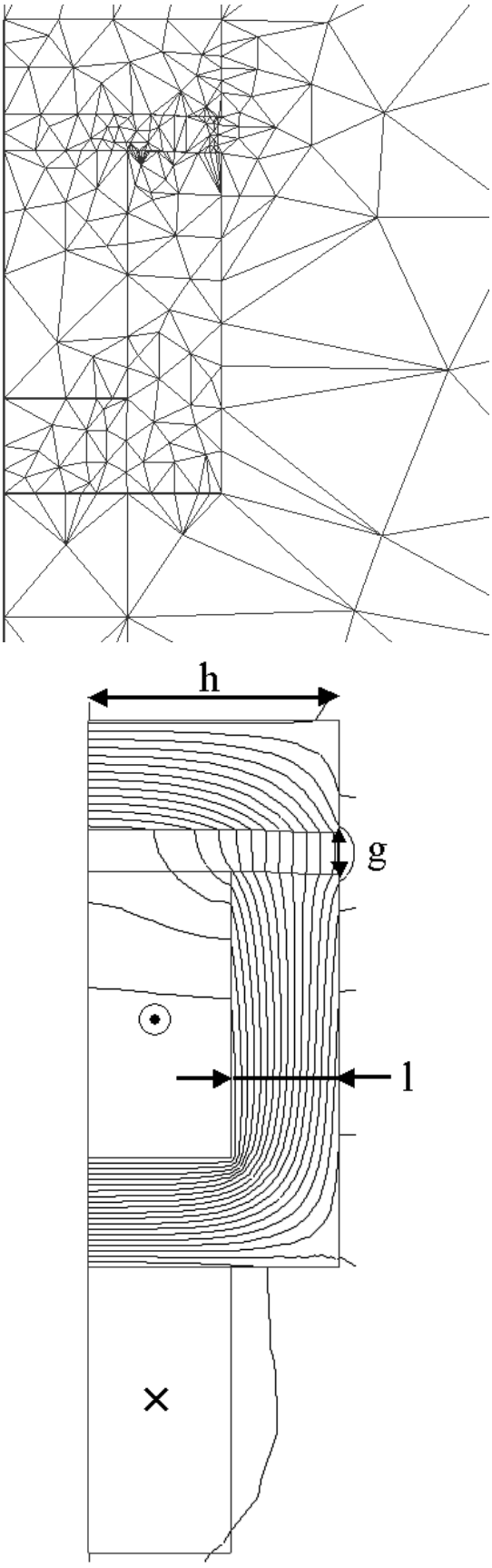

Figure 4: Detail of: a - finite element mesh , b - field solution

eddy current effect has been neglected. Although the behavior of the electromagnet is time-dependent, the steady state condition is considered, just to take into account the worst case for the design. Resorting to finite element method, the computational domain has been discretized in a mesh composed of about 500 triangular elements, as is shown in Figure 4a. The boundary conditions are expressed in terms of magnetic vector potential A as $\partial A/\partial n = 0$ along the symmetry axis of the device and $A = 0$ elsewhere. Given the current density in the winding, Poisson's equation of the vector potential in two dimensions is solved, taking into account the nonlinear characteristic of iron; a typical field solution is represented in Figure 4b. At a given current density, the electromagnetic force F acting on the plunger depends strongly on its position and, therefore, on the magnetization of iron. In particular, the force-stroke curve is obtained by applying the virtual work principle

$$F = \frac{\partial W}{\partial g}$$

where W is the co-energy of the system and g is the displacement of the plunger with respect to the core; the derivative is approximated by finite difference taking $\Delta g = 1mm$ as discrete displacement. For each position of the plunger the mesh is generated again, and the field analysis is repeated. To speed up the computation of the electromagnetic force, a lumped parameter model of the electromagnet has been adopted. Therefore, a non-linear magnetic circuit has been considered, in which the equivalent reluctance

$$R_{eq} = \frac{4h}{\mu_0 \mu_r l^2} + \frac{2g}{\mu_0 l^2}$$

varies according to the position g of the plunger, l being the diameter of the core cross-section and h being the length of the plunger. The relative permeability of iron $\mu_r = \frac{dB}{dH}$ is to be evaluated according to the following expression:

$$B = \beta_1 (1 - e^{\frac{\beta_2 H}{\beta_3}}) + \mu_0 H$$

where B is the flux density, with $\beta_1 = 1.586690$ [T], $\beta_2 = 1.892574$, $\beta_3 = 399.997068$ [A/m] and $\mu_0 = 4\pi 10^{-7}$ [H/m]. The latter model represents with acceptable accuracy the constitutive relation of laminated iron around saturation. For a given g, the circuit equation is solved by applying the bisection method; the iterative procedure is stopped when the residual r of Ampère's equation

$$r = J(h-l)^2 - \left(\frac{B}{\mu_0 \mu_r} 4h + \frac{B}{\mu_0} 2g \right)$$

is less than a prescribed tolerance. The force is then evaluated as:

$$F = \frac{1}{2} J^2 (h-l)^4 \frac{d}{dg}(R_{eq}^{-1}) \tag{8}$$

The dependence of force F on position g is shown in Figure 5; the validity of the circuit approach is assessed by means of field analysis ([14]). In the followings, all computations have been carried out by means of the circuit model.

In view of the design problem, geometric parameters h and l are selected as design variable vector $\mathbf{x}$, subject to suitable bounds. A constraint on the maximum temperature rise by the winding has been introduced. The optimization aims at identifying the shape of the electromagnet such that:

- the force $f_1(\mathbf{x}) = F$ on the plunger is maximum for the position $g = 10$[mm],

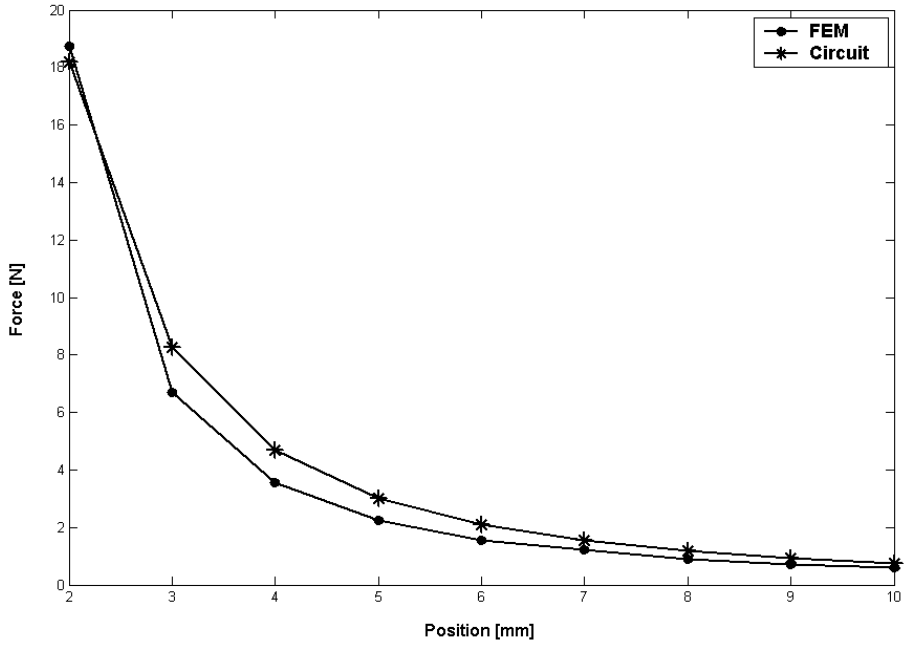

Figure 5: Force *vs.* displacement curve of the electromagnet.

- the power loss $f_2(\mathbf{x}) = \frac{\pi h J^2 f t_{on}}{\sigma}$ in the winding is minimum, where $\sigma = 6 \cdot 10^7$ [S/m] and $t_{on} = 80$ [ms], $f = 6Hz$,
- the cost $f_3(\mathbf{x}) = c_1 V_1 + c_2 V_2$ of materials is minimum, where $c_1 = 1$, $c_2 = 3$, V_1,V_2 are the costs per unit and the volumes of iron and copper, respectively.

It can be easily seen that two of the three objectives are cooperative, namely the power loss and the cost of materials, whist the first objective does conflict with them. Therefore, it has been decided to cast the following multi-objective optimization problem:

$$\begin{cases} \min\limits_{\mathbf{x}\in\Omega} \mathbf{f} = \{f_1(\mathbf{x}), f_3(\mathbf{x})\} \\ \text{subject to the problem contraints} \end{cases} \tag{9}$$

6 Results and conclusion

By applying the methodology described in section 2, the results reported in Figures 6 and 7 were obtained.

As a reference for comparison, a non-dominated set in the objective space was taken, ensuing from a very large sampling of the feasible region (hereinafter called exact front). Due to the very low sensitivity to variable l, the POS nearly coincides with the upper border of the feasible region. The proximity of the POS towards the search space border is a difficulty for the presented optimization algorithm for the following two reasons:

- The evolutionary engine may find difficulties when approaching the borders of the feasible region [15],
- The NN interpolation error is often higher in the search space border regions.

This is why the presented test case seems to give good testing for a GRS-MOEA strategy.

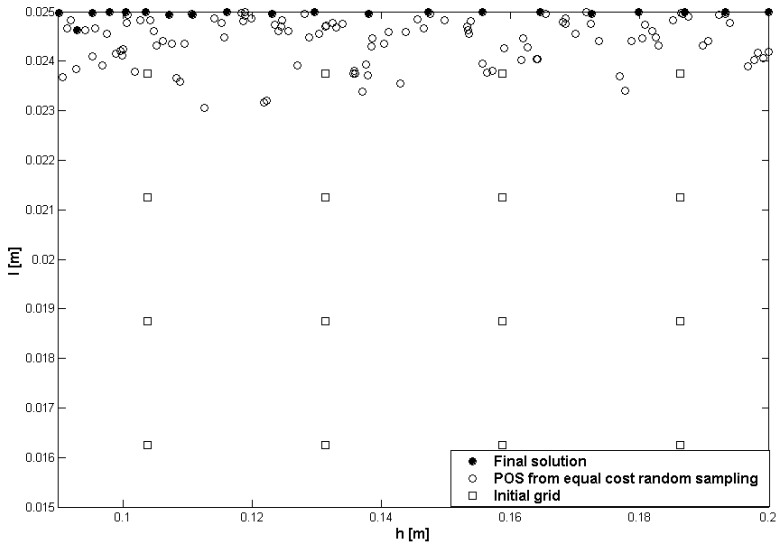

Figure 6: Compared Pareto Optimal Sets and initial NN-training grid.

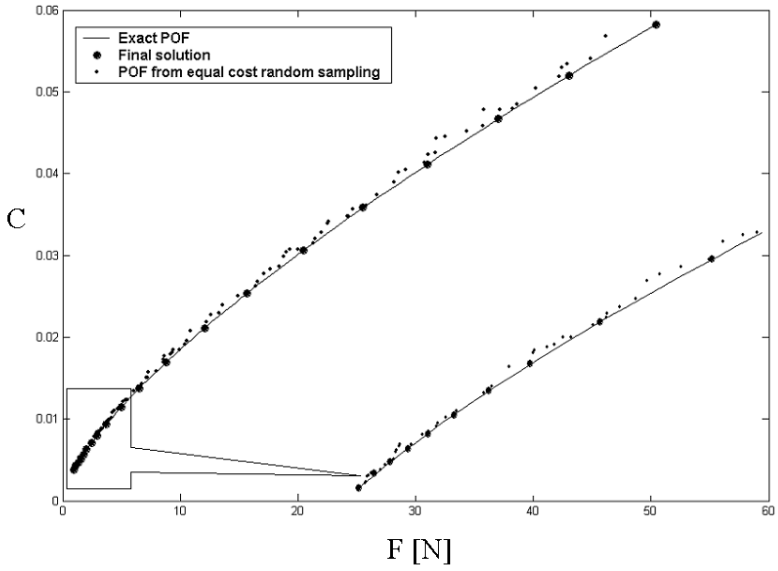

Figure 7: Compared Pareto Optimal Fronts: global view and zoom of a detail.

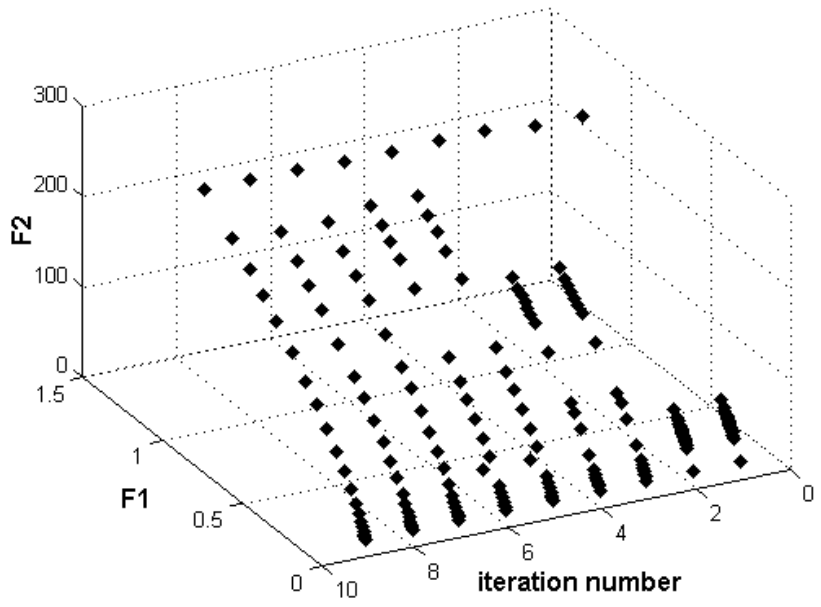

Figure 8: Story of the POF approximation.

The story of the POF interpolation is presented in figure 8; in the first iterations the method performs a global refinement of the approximation while a local refinement is performed toward the end of the overall iterative process.

The final front from the optimization (total cost: 120 true objective function evaluation), shows to overlap with the exact front in fairly good agreement. One could argue that the observed good accuracy may depend on low sensitivity to the design variables, in the proximity of the optimal region; actually, the two sets are well overlapped also in the X space. As is typical of many MO problems, individuals spanning the POS quite uniformly in the X space – as is the case here – map into a definitely non-uniform sampling of the POF. In fact, the zoom evidences the crowding of points in the F space, towards the left end of the front. Finally, for the sake of comparison, a uniform sampling in terms of true objective function evaluation was taken in the feasible region; the POS and POF so extracted evidence a strong discrepancy to the reference case. Therefore, one may conclude that the optimization method here proposed has been successfully applied.

References

[1] U. Pahner and K. Hameyer, "Adaptive coupling of differential evolution and multiquadrics approximation for the tuning of the optimization process," *Proceedings of COMPUMAG Sapporo*, pp. 116–117, October 25-28 1999.

[2] G. Molinari P. Alotto, M. Gaggero and M. Nervi, "A design of experiment and statistical approach to enhance the generalised response surface method in the optimisation of multi-minima problems," *IEEE Trans. Mag.*, vol. 33, no. 2, pp. 1896–9, 1997.

[3] Z. Malik H. Su J. Nelder R. Rong, D. Lowther and R. Spence, "Applying response surface methodology in the design and optimisation of electromagnetic devices," *IEEE Trans. Mag.*, vol. 33, no. 2, pp. 1916–9, 1997.

[4] A. H. Al-Khoury J. K. Sykulski and K. F. Goddard, "Minimal function calls approach with on-line learning and dynamic weighting for computationally intensive design optimisation," *Proccedings of IEEE CEFC'2000*, June 2000.

[5] E. Zitzler and K. Deb et al. editors, *Evolutionary Multi-Criterion Optimization, proceedings of EMO2001, Zurich*, vol. 1993, 2001.

[6] K. Deb, "Nonlinear goal programming using multi-objective genetic algorithms," *PJournal of the Operational Research Society*, vol. 52, no. 3, pp. 291–302, 2001.

[7] M. Farina, "A minimal cost hybrid strategy for pareto optimal front approximation," *Evolutionary Optimization, , (2002)*, vol. 3, no. 1, pp. 41–52, 2001.

[8] K. Miettinen, *Nonlinear Multiobjective Optimization*, Kluwer Academic Publishers, Dordrecht, THE NEDERLANDS, 1999.

[9] Y. Rahmat-Samii and Eric Michielssen, *Electromagnetic Optimization by Genetic Algorithms*, Wiley, New York, 1999.

[10] K. Rashid, M. Farina, J.A. Ramirez, J.K. Sykulski, and E.M. Freeman, "A comparison of two generalized responce surface methods for optimization in electromagnetics," *COMPEL*, vol. 3, no. 20, pp. 741–752, 2001.

[11] M. Farina and J.K. Sykulski, "Comparative study of evolution strategies combined with approximation techniques for practical electromagnetic optimization problems," *IEEE Trans. Mag.*, vol. 37, pp. 3216–3220, 2001.

[12] A. Bramanti, P. Di Barba, M. Farina, and A. Savini, *Combining Response Surfaces and Evolutionary Strategies for Multiobjective Pareto-Optimization in Electromagnetics*, vol. 9 of *Studies in Applied Electromagnetics and Mechanics*, JSAEM, Tokyo, 2001.

[13] M. Farina, "A neural network based generalized response surface multiobjective evolutionary algorithm," *Proceedings of IEEE-CEC2002 Honolulu, USA 12-17 July 2002*, 2002.

[14] Infolytica Corporation, "MagNet Version 6, Getting Started Guide," *http://www.infolytica.com*, 1999.

[15] C.A. Coello Coello, "A survey of constraint handling techniques used with evolutionary algorithms," *http://www.lania.mx/ ccoello/EMOO/EMOObib.html*.